JOURNAL OF VIROLOGY, June 1993, p. 2961–2971
0022-538X/93/062961-11$02.00/0

Vol. 67, No. 6

Biochemical and Genetic Evidence for a Pseudoknot Structure at the 3′ Terminus of the Poliovirus RNA Genome and Its Role in Viral RNA Amplification

SANDRA J. JACOBSON,[1]† DANIELLE A. M. KONINGS,[2] AND PETER SARNOW[1]*

Department of Biochemistry, Biophysics and Genetics, University of Colorado Health Sciences Center, Denver, Colorado 80262,[1] and Department of Molecular, Cellular, and Developmental Biology, University of Colorado, Boulder, Colorado 80309

Received 23 December 1992/Accepted 19 February 1993

The sequences in the plus-stranded poliovirus RNA genome that dictate the specific amplification of viral RNA in infected cells remain unknown. We have analyzed the structure of the 3′ noncoding region of the viral genome by thermodynamic-based structure calculation and by chemical and enzymatic probing of in vitro-synthesized RNAs and provide evidence for the existence of an RNA pseudoknot structure in this region. To explore the functional significance of this structure, revertants of a mutant bearing a lesion in the proposed pseudoknot and exhibiting a temperature-sensitive defect in viral RNA synthesis were isolated and mapped. The results of this genetic analysis established a correlation between the structure of the 3′ terminus of the viral RNA and its function in vivo in RNA amplification. Furthermore, phylogenetic analysis indicated that a similar structure could be formed in coxsackievirus B1, a related enterovirus, which further supports a role for the pseudoknot structure in viral RNA amplification in infected cells.

The plus-strand poliovirus RNA genome is 7,440 nucleotides (nt) long and encodes a polyprotein with a relative molecular weight of 220,000 (17, 27). The coding region is flanked by 5′ and 3′ noncoding regions (NCRs) that have unusual properties. The 750-nt 5′ NCR contains sequence elements that mediate translation initiation by internal ribosome binding (21) and, by specifying the sequences at the 3′ end of the minus strand, initiation of plus-strand RNA (for a review, see reference 28). The 65-nt 3′ NCR is highly conserved among the enteroviruses (38) and is likely to bear sequences involved in the initiation of minus-strand RNA synthesis. Although the poliovirus polymerase 3D selectively amplifies the viral genome in vivo, it has been shown previously that soluble 3D will nonselectively copy any polyadenylated RNA molecules in vitro when provided with an oligouridylate primer (12) or a 68-kDa cellular protein (10).

To understand the molecular mechanism underlying the initiation of minus-strand viral RNA synthesis in infected cells, we have analyzed the structure and function of the viral 3′ NCR by biochemical and genetic approaches, respectively. First, thermodynamic-based structure calculation followed by chemical and enzymatic probing of in vitro-synthesized viral RNAs pointed to the existence of a pseudoknot (PK) structure in the viral 3′ NCR. Second, formation of the predicted PK for several mutant RNA genomes correlated with the capability of viral genomes to initiate RNA synthesis in infected cells. Finally, phylogenetic analysis provided evidence that a similar PK structure could form in the 3′ terminus of coxsackievirus B1. These observations indicate that this structure may be an important element in the amplification of RNA molecules in enterovirus-infected cells.

* Corresponding author.
† Present address: Department of Molecular Biophysics & Biochemistry, Yale University School of Medicine, New Haven, CT 06536.

MATERIALS AND METHODS

Thermodynamic calculation of RNA secondary structure. Optimal and suboptimal foldings were calculated through minimization of free energy by using the algorithm described by Zuker (41). For each sequence analyzed, multiple suboptimal foldings were generated with different window sizes (i.e., the distance of the structural difference between subsequently generated suboptimal foldings; up to a window size of 10) and within 10% energy difference to the energy of the optimal structure. The set of free-energy values given by Jaeger et al. (16) was used in the analysis.

Enzymes and RNA transcription vectors. Enzymes used for cloning and polymerase chain reaction (PCR) were purchased from Promega Biotec. Cobra venom nuclease V1 and RNase PhyM were purchased from Pharmacia. RNase A and RNase T_1 were obtained from Bethesda Research Laboratories. All pGEM and pSP transcription vectors were purchased from Promega Biotec.

Oligodeoxynucleotides. Oligonucleotide $3'ncr_{(C')}$ (5′-CTC CGAATTAAAGA-3′) is complementary to the terminal 14 nt (nt 7440 to 7427) of plus-sense poliovirus RNA. Oligonucleotide $3'ncr_{(C')}$-*Sac*I (5′-AAAGAGCTCCGAATTAAAG AAAAA-3′) is complementary to the terminal 18 nt (nt 7440 to 7423) of plus-sense poliovirus RNA and contains a *Sac*I restriction enzyme site (underlined) at its 5′ end. Oligonucleotide $5504_{(S)}$ (5′-GGAGAGTTCACTATGTTAGGAGT C-3′) is identical to sequences 5504 to 5527 of the poliovirus genome. The sequence for the T7 promoter oligonucleotide is 5′-TAATACGACTCACTATAGGG-3′, and that for the PK1 oligonucleotide is 5′-GGTTGCCGAACCCAATATT CATTTTTAGTAACCC-3′ (mutant residues are underlined).

Construction of DNA templates used for in vitro transcription. To generate an RNA transcript containing the 3′-terminal, 1,830-nt wild-type Mahoney type 1 poliovirus sequences, full-length viral cDNA was used as a template to amplify a 1.9-kb DNA segment by PCR with oligonucleotides $5504_{(S)}$ and $7440_{(C')}$-*Sac*I as primers. The amplified

fragment was cut with *Bgl*II (nt 5601) and *Sac*I and cloned into the *Bam*HI and *Sac*I sites, located downstream of the T7 promoter, of pGEM4polyA [a derivative of pGEM4 containing a *Sac*I-*Eco*RI poly(A) cassette from the pSP64polyA vector]. The resulting clone, T7-WT B/S pA, contains poliovirus sequences from nt 5601 through the 3′ NCR (17, 27) followed by a *Sac*I site, a poly$(A)_{30}$ cassette, and an *Eco*RI site.

To generate RNA transcripts containing the 3′-terminal 924, 135, and 108 nt of poliovirus, three derivatives of full-length T7D-poliovirus (31) were constructed. An important feature of these clones is an A_{12} cassette immediately downstream of the 3′ NCR followed by a unique *Mlu*I restriction site. Therefore, plasmids linearized with *Mlu*I yielded RNA transcripts with 3′ ends similar to those of virion RNA but ending in only 12 adenosines followed by 4 extra nucleotides. In vitro synthesis of RNA by T7 RNA polymerase was as described previously (31).

T7-3NC202 B/S pA and T7-R9 B/S pA contained a *Bgl*III (position 5601 in the poliovirus RNA)-to-*Sac*I fragment (located at the 3′ end; see above) bearing the mutations of 3NC202 and R9, respectively, in the *Bam*HI and *Sac*I sites of vector pGEM4polyA.

PK1pA was constructed by using PK1 and 3′$ncr_{(C')}$ oligonucleotides to generate DNA containing the desired mutations from nt 7358 to 7366 in an 80-bp fragment by PCR. The mutagenized DNA was gel isolated and cloned into a *Hin*cII site in pGEM5Zf(+). This plasmid was then cut with *Pst*I and *Sac*I in the polylinker flanking the poliovirus sequences, and this fragment was cloned into pGEM4polyA at these sites.

Chemical and enzymatic probing of RNA. RNA structure analysis was performed as described by Moazed et al. (20) and Stern et al. (35). TMK buffer is 30 mM Tris-HCl (pH 7.4)–10 mM $MgCl_2$–270 mM KCl in diethylpyrocarbonate-treated H_2O.

(i) Modification and enzymatic treatment of RNA followed by primer extension analysis. A 30-μl TMK buffer solution containing 30 μg of poliovirus RNA transcript was supplemented with 18 mM 2-mercaptoethanol and 100 μg of *Escherichia coli* tRNA (Sigma), heated to 68°C for 5 min, slowly cooled to 37°C, placed on ice, and treated with enzymes and chemicals as described previously (20, 35). Forty nanograms of 5′ ^{32}P-end-labeled oligonucleotide 3′$ncr_{(C')}$ was added to treated and untreated RNA, and the annealed primers were extended by avian myeloblastosis virus reverse transcriptase (Life Sciences) (4). Samples were analyzed in 8% acrylamide–7 M urea gels.

Dideoxy sequencing of untreated, primer-extended RNA was done according to the method of Zaug et al. (40), and samples were analyzed in parallel with probed RNA samples by electrophoresis in polyacrylamide-urea gels.

(ii) Enzymatic treatment and analysis of 5′ ^{32}P-end-labeled RNA. RNA was denatured and renatured in TMK buffer as described above, except that 30 μg of tRNA was added. About 2 μg of ^{32}P RNA was preincubated in 7 μl of TMK buffer on ice and digested with cobra venom nuclease V1 (0.05 U for 20 min), RNase A (28 ng/ml for 15 min), or RNase T_1 (2×10^{-4} U for 15 min). Reactions were stopped by the addition of 8 μl of 10 M urea. Samples were heated at 90°C for 3 min and loaded directly onto an 8% polyacrylamide–7 M urea gel.

5′ ^{32}P-end-labeled poliovirus RNA was enzymatically sequenced according to the method of Donis-Keller (11).

Cells and viruses. HeLa cells were grown in Dulbecco's modified Eagle's medium supplemented with 10% bovine serum (Irvine Scientific). High-titer stocks of wild-type Mahoney type 1 poliovirus were grown in HeLa cells at 37°C, stocks of mutant 3NC202 virus were grown in HeLa cells at 32.5°C, and stocks of revertant viruses were grown in HeLa cells at 39.5°C.

Isolation, cloning, and sequencing of revertant polioviruses. PFU (2×10^6) of 3NC202 virus in 100 μl of phosphate-buffered saline were applied to a HeLa cell monolayer, adsorbed at 37°C for 30 min, overlaid with 1% agar (Difco), and incubated at the nonpermissive temperature of 39.5°C for 60 h. Eight individual plaques (of approximately 100 visible plaques) were picked and plaque purified three times (33) on HeLa cells at 39.5°C.

To generate revertant virion cDNA, virion RNA was isolated from purified revertant virions. First-strand cDNA synthesis was performed as described previously (4) with the 3′$ncr_{(C')}$ oligonucleotide as a primer. To generate double-stranded cDNA, first-strand cDNA was amplified by PCR in a 100-μl reaction volume with oligonucleotides $5504_{(S)}$ and 3′$ncr_{(C')}$-*Sac*I as primers. Amplified, 1.9-kb DNA was isolated, cut with *Bgl*II and *Sac*I, and cloned into the corresponding sites of plasmid pSP72. The sequence of the 3′-terminal 100 nt was verified by sequencing of in vitro-synthesized RNAs (4).

To verify that the sequence changes in the revertant 3′ NCRs were sufficient for the restoration of RNA synthesis at 39.5°C, the genotype of revertant R5, bearing an AC dinucleotide at nt 7386 and 7387, was introduced into a wild-type full-length cDNA by directed mutagenesis (9). This recombinant virus yielded the expected phenotype. The additional revertant genotypes, listed in Fig. 7, were not reconstructed into wild-type full-length cDNAs. Thus, we cannot rule out the possibility that secondary lesions in these genomes contributed to the revertant phenotypes. However, this is unlikely, considering that the nucleotide changes in the revertant genomes occurred at similar nucleotide positions.

Measurement of viral RNA synthesis. Measurement of viral RNA synthesis was performed as described previously (33) except that HeLa cells were infected with wild-type, 3NC202, or revertant virus at multiplicities of infection of 20 and were incubated at 39.5°C. Positive-sense viral RNA bound to nitrocellulose filters was detected by hybridization to in vitro-synthesized ^{32}P-labeled minus-sense RNA that was complementary to poliovirus sequences at nt 6516 to 7205.

RESULTS

Thermodynamic-calculated RNA folding patterns of the poliovirus 3′ NCR. To investigate the structure of the 3′ NCR of poliovirus RNA, computer-aided RNA structure analysis was performed on an RNA sequence representing the 3′-terminal 122 nt of poliovirus genomic-sense RNA with a computer algorithm designed to generate optimal and suboptimal secondary structures based on free-energy minimization (41) (see Materials and Methods). Because in vitro biochemical structure probing of an analogous RNA yielded a pattern of chemical and enzymatic reactivity similar to that of full-length poliovirus (see below), we chose to concentrate on this small RNA for computational analysis to investigate in detail alternative RNA structures in the 3′ NCR that exhibit significant variation in folding. Three different folding conformations were generated for the viral 3′ NCR (nt 7376 to 7440; Fig. 1), while the 45 nt 5′ to the 3′ NCR (nt 7330 to 7375) showed more structural variation. The RNA structure with the lowest free energy is shown in Fig. 1A, and to

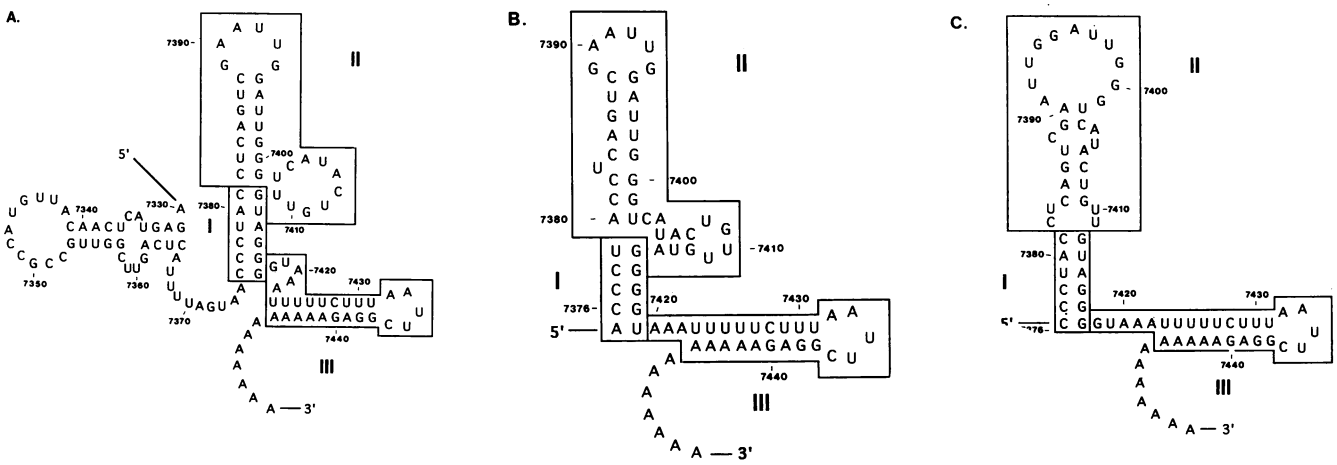

FIG. 1. Computer-predicted RNA folding of the 3′ terminus of positive-strand Mahoney type 1 poliovirus RNA. For comparison, three elements (boxed and labeled I, II, and III) are defined by their respective helical segments. Every 10th nucleotide is numbered according to its position in full-length genomic RNA. The 3′ NCR extends from C-7376 (in element I) to G-7440 (in element III). A poly(A) tail of 12 residues is illustrated, although it is of heterogeneous length in virion RNA. (A) Secondary structure of the terminal 122 nt of poliovirus RNA with the lowest free-energy value (ΔG = −23.7 kcal/mol) (ca. −99.1 kJ/mol); (B and C) alternative foldings of the 3′ NCR. Folding upstream of the 3′ NCR (not shown) is the same as in panel A. Predicted ΔG values are −21.9 and −21.4 kcal/mol (ca. −91.2 and −90 kJ/mol), respectively.

simplify comparison, three regions in the 3′ NCR (beginning with nt 7376) are labeled I, II, and III and are defined by their respective helical segments. The conformations in Fig. 1A and C versus that in Fig. 1B show a slightly shifted structural element I; the conformations in Fig. 1A and B versus that in Fig. 1C display variation in structural element II, while element III is invariant in all three conformations (Fig. 1).

In vitro chemical and enzymatic probing supports the presence of a hairpin structure in the viral 3′ NCR. To distinguish between these possible RNA conformations, RNA secondary structure analysis of the 3′ NCR of the poliovirus genome was performed by chemical and enzymatic probing. In a first attempt, we chose a long RNA as a probing substrate to allow for potential long-range RNA-RNA interactions that may contribute to the structure of the 3′ NCR. Thus, a transcript 1,800 nt in length was made in vitro by T7 RNA polymerase. This transcript (designated T7-WT B/S pA) contained 1,700 nt of the P3 region followed by the 65-nt viral 3′ NCR, followed by 6 nt derived from a *Sac*I restriction site present in the DNA and a 3′-terminal poly(A) tail (Fig. 2). The secondary structure of the transcript was analyzed with chemicals and enzymes that react selectively with single-stranded (dimethylsulfate [DMS], RNase A, and RNase T_1) or helical (cobra venom nuclease V1) regions in RNA (see Materials and Methods).

Figure 3 shows an autoradiograph of such an analysis. Three major areas displayed consecutive nucleotides that were susceptible to single-strand-specific reagents: (i) G-7372, U-7373, A-7374, and A-7375, (ii) C-7388, G-7389, and A-7390, and (iii) G-7399, G-7400, G-7401, C-7403, A-7404, U-7405, and A-7406 (Fig. 3, lanes 2, 4, and 5). Residues G-7418 through A-7422 were also susceptible to cleavage by single-strand-specific probes when samples were analyzed on a higher-percentage denaturing polyacrylamide gel (not shown) and are presented in parentheses in Fig. 4. These single-stranded regions flank a stretch of 6 contiguous bp (element I, Fig. 4) that are in a helical conformation, as shown by helical RNA-specific V1 cleavage at nt C-7378, U-7379, C-7384, and A-7385 (Fig. 3, lane 3) and at nt G-7415 and G-7416 (Fig. 4). These V1 cleavage sites are consistent with each of the three folding patterns in Fig. 1 in which C-7378/U-7379 and C-7384/A-7385 participate in the helices of elements I and II, respectively. However, the susceptibilities of G-7399, G-7400, and G-7401 to RNase T_1, indicating that they are unpaired, are inconsistent with the foldings in Fig. 1A and B. In contrast, G-7399, G-7400, and G-7401 are predicted to be unpaired in Fig. 1C. Furthermore, C-7388 and G-7395 are susceptible to DMS and RNase T_1, respectively, although they are predicted to be base-paired to each other in Fig. 1A and B. Therefore, these data are most consistent with the conformation shown in Fig. 1C. However, the predicted base pairings between G-7389/C-7403 and A-7390/U-7402 are apparently present in a breath-

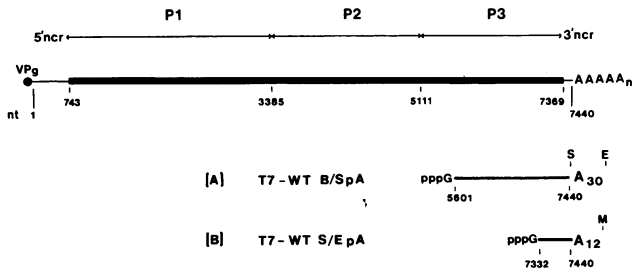

FIG. 2. Illustration of poliovirus RNA transcripts used for in vitro RNA structure analysis. (Top) Schematic representation of the 7,440-nt poliovirus genomic RNA. The thin lines denote the NCRs, the thick bar denotes the coding region, the filled circle denotes the genome-linked virion protein (VPg), and A_n denotes the heterogeneous poly(A) tail. The P1 region encodes structural proteins; the P2 and P3 regions encode nonstructural proteins. (A) Diagram of T7-WT B/S pA RNA, consisting of poliovirus sequences 5601 to 7440 followed by a poly(A) tail of approximately 30 nt and an additional 7 nt of heteropolymer derived from the *Eco*RI linearization site. Restriction sites present in the cDNA are indicated (S, *Sac*I; E, *Eco*RI). Structural analysis of this RNA is shown in Fig. 3. (B) Diagram of T7-WT S/E pA RNA, consisting of poliovirus sequences 7332 to 7440 followed by a poly(A) tail of 12 nt and 4 nt derived from the *Mlu*I linearization site.

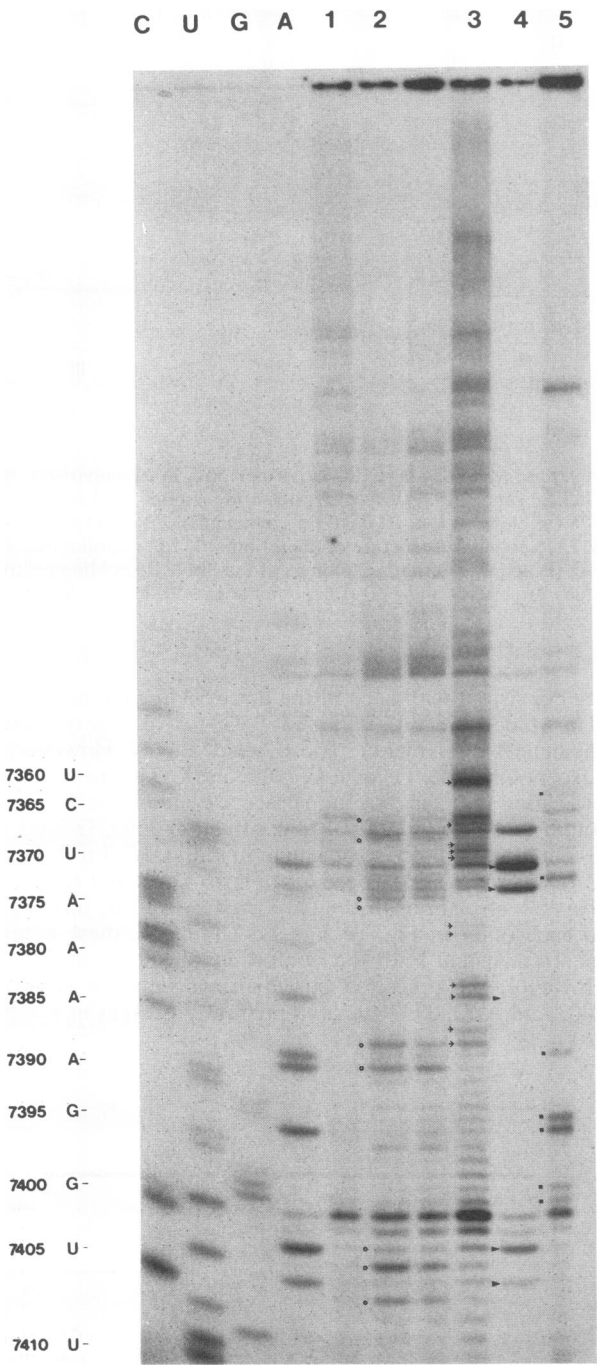

FIG. 3. Structural analysis by chemical and enzymatic probing of in vitro-synthesized poliovirus RNA. T7-WT B/S pA RNA [1.8-kb poly(A)$_{30}$ RNA (Fig. 2A)] was treated as described in Materials and Methods, annealed to a ^{32}P-5′-end-labeled oligonucleotide complementary to the terminal 14 nt of the 3′ NCR, and then transcribed with reverse transcriptase. The elongation products were separated on a urea-containing polyacrylamide gel; an autoradiograph, a representative of many such gels, is shown. The nucleotide sequence of the RNA as deduced from the dideoxy sequencing lanes (labeled on top) is indicated on the left. Lanes: 1, untreated RNA; 2, DMS (○); 3, cobra venom nuclease V1 (→); 4, RNase A (▲) (20 ng/ml); 5, RNase T_1 (■). RNA residues showing significant probe reactivity in this and several other such experiments are marked by the appropriate symbol to the left of the lane. Note that because of the nature of these modifications, primer-extended DNA fragments stop 1 base short of the corresponding reactive residue as read on the dideoxy sequencing ladder. However, V1 cleavages yield primer extension products that comigrate with the same residue seen in the sequencing reaction.

ing (partly open and closed) or an alternative interaction, as demonstrated by the susceptibilities of G-7389, C-7403, and A-7390 to single-strand-specific probes. Therefore, the data support the presence of an RNA hairpin in the 3′ NCR which incorporates elements I and II as presented in Fig. 4, beginning just downstream of the translational termination codons and ending at G-7417. The structure(s) in the loop of this hairpin was difficult to assess from these data; however, the stem structure is in good agreement with those proposed by Iizuka et al. (14) and Pilipenko et al. (23), which are based primarily on phylogenetic comparisons of related picornaviruses.

To confirm the presence of this RNA hairpin further and to determine the structure of the very 3′ terminus of the 3′ NCR (i.e., element III), enzymatic probing of a short 5′ ^{32}P-end-labeled 132-nt RNA was performed (designated T7-WT S/EpA in Fig. 2). This RNA differed from T7-WT B/S pA in several respects: (i) it contained 38 rather than 1,700 nt upstream of the 3′ NCR, (ii) it contained no additional nucleotides between the 3′ NCR and the poly(A) tail, and (iii) the poly(A) tail was 12 rather than 30 nt long. Figure 5 shows a typical enzymatic cleavage pattern of 5′-end-labeled T7-WT S/E pA RNA (lanes 1 to 4) run in parallel with enzymatically sequenced RNA (lanes 5 to 7). The RNase T_1 cleavage sites (lane 4) were identical to those in T7-WT B/S pA (Fig. 3) except for a very weak recognition of G-7386 and of the three terminal G residues (G-7437, G-7438, and G-7440) in the 3′ NCR which could not be assigned by primer extension analysis. RNase A cleaved strongly at C-7365, U-7370, U-7373, and C-7403 (lane 3) and cleaved weakly at U-7379, C-7384, U-7405, and U-7413. Strong RNA cleavage sites at C-7365, U-7370, U-7373, and C-7403 were difficult to interpret, because the same sites were preferentially cleaved in non-RNase A-treated RNA (lane 1). However, nt U-7370, U-7373, and C-7403 were clearly RNase A sensitive by primer extension analysis of T7-WT B/S pA (Fig. 3, lane 4). The V1 digestion pattern (Fig. 5, lane 2) was also similar to that of T7-WT B/S pA; the characteristic hits at U-7360, C-7365, U-7367/U-7368, C-7378, C-7384/A-7385, and C-7388/G-7389 were all present. Three other sets of V1 hits were observed at the very 3′ terminus of the 3′ NCR. The strong triplet at G-7415, G-7416, and G-7417, at the base of the predicted stem, further demonstrated the stable C-G base pairing here (Fig. 4). Note that even in the RNase T_1 sequencing reaction mixture (Fig. 5, lane 6), treated with the same amount of enzyme but digested under denaturing conditions, these three residues were not hit by T_1. The two V1 sites at C-7428 and U-7429, plus the strong V1 hit within the poly(A) tail, could be explained by base pairing of the poly(A) tail with the upstream uridines (nt 7423 to 7431). This possibility is also supported by the recurrence of this base-pairing arrangement in the computer-generated structure analysis (Fig. 1, element III). In addition, the similar patterns of probe reactivity exhibited by T7-WT S/E pA and T7-WT B/S pA demonstrate that upstream 5′ sequences do not exert a significant influence on the secondary structure of the 3′ NCR. This conclusion has been confirmed further by chemical and enzymatic probing of RNA transcripts bearing 165 and 854 nt upstream of the 3′ NCR as well as full-length genomic-sense viral RNA (data not shown).

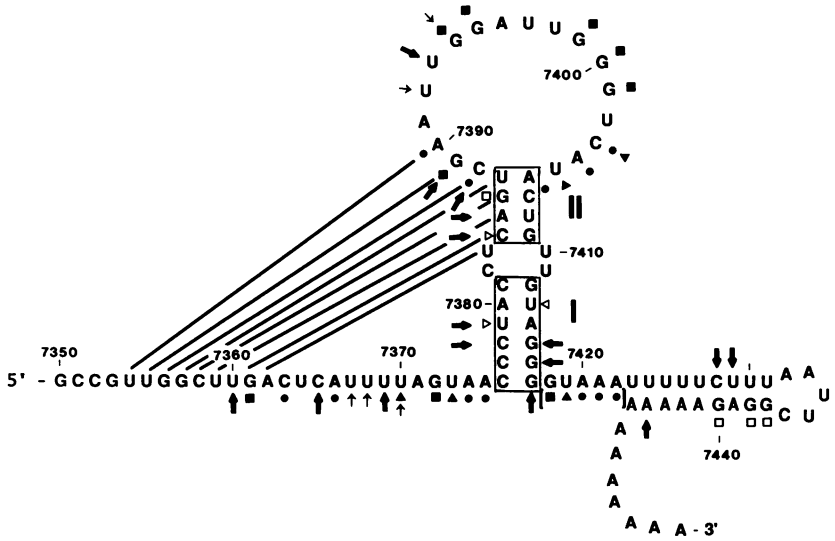

FIG. 4. Proposed stem-loop structures in the 3′ NCR of poliovirus. Nucleotides reactive to treatment with DMS (●), cobra venom nuclease V1 (⟶), RNase A (▲), and RNase T_1 (■) are marked. Thick and thin arrows indicate nucleotides with strong and weak reactivities, respectively, to cobra venom nuclease treatment. Alternative base pairing of nt 7383 to 7390 with nt 7354 to 7362 is indicated by diagonal lines.

Evidence for the presence of an RNA PK existing in equilibrium with the RNA hairpin. There are several observations that are not apparently compatible with a simple hairpin model. First, nt 7360 to 7370 exhibit discrete and relatively strong V1 sites in the absence of obvious base-pairing partners in the single-stranded regions upstream of nt U-7360 or downstream of nt G-7418. Second, nt C-7388/G-7389 and G-7394 show dual sensitivities in that they are susceptible to both V1 nuclease and to single-strand-specific probes. One explanation for these observations could be the existence of higher-order folding in the RNA structure, in which nt U-7354 through A-7362, upstream of the hairpin, base pair with nt U-7383 through A-7390 in the hairpin loop (solid lines in Fig. 4), forming a PK-like structure. A classic PK is formed when unpaired residues in a hairpin loop base pair with complementary nucleotides outside of the loop, resulting in stabilizing coaxial stacking of the two stems into an extended type A helix (25, 26). The proposed PK in the poliovirus 3′ NCR is drawn in Fig. 6 to show the analogy to this base-pairing arrangement; the base pairing of nt 7354 to 7362 with nt 7382 to 7390 creates a new stem (S1) adjacent (separated by a C residue) to the lower 6 bp of the hairpin stem (S2).

The locations of the V1-reactive sites within stem S1 support an interaction between nt 7354 to 7362 and 7383 to 7390 (Fig. 4). First, the C-7388/G-7389 cleavages may result from the ability of V1 to bind to stacked duplex regions and cleave 1 or 2 nucleotides 3′ to its binding site (3). Second, V1 cleaved C-7384/A-7385 and U-7360, which lie directly across from each other in the helix. The very strong V1 cleavage at U-7360 may reflect the ability of V1 to induce one cleavage at a time in the RNA duplex (3, 18). Finally, the V1 sites at U-7367/U-7368/U-7369/U-7370 in loop I could arise from base pairing with adenosine residues of the poly(A) tail, possibly as a result of being displayed in loop I of the PK structure (Fig. 6). This is supported by in vitro RNA structure analysis of 3′-terminal poliovirus transcripts, lacking a poly(A) tail, which clearly exhibited a specific loss of these V1 sites (data not shown). Because V1 cleavages were seen at nt C-7428 and U-7429 and within the poly(A) tail in poly(A)-containing RNA (Fig. 3 and 5), these data support a model in which the poly(A) tail forms an extended helix by initially base pairing with the proximal uridine stretch, bypassing the base of stem S2, and resuming pairing with the uridines at nt 7367 to 7370 in loop I of the PK (Fig. 6). A terminal poly(A) tract in genomic poliovirus has been previously thought to confer stability to the genome in the host cell (31, 34). These data suggest that the poly(A) tract is base paired to upstream pyrimidine sequences in the 3′ terminus of the poliovirus genome.

Genetic analysis of the function of the viral PK in the virus life cycle. To provide evidence for the PK structure in full-length viral RNA molecules and to test the functional significance of this structure in the viral life cycle, revertants of a mutant bearing a lesion in the predicted PK structure were isolated and studied.

We have previously reported the construction and isolation of a poliovirus mutant, designated 3NC202, that bears an 8-nt insertion in the 3′ NCR of the viral genome (32). This mutant displayed a temperature-sensitive phenotype for growth at 39.5°C because of its inability to synthesize RNA at the nonpermissive temperature (32). Furthermore, this mutant could not be complemented by coinfection with other well-defined poliovirus mutants (5), demonstrating the *cis*-acting nature of the mutation within the 3′ NCR. That the 8-nt insertion at nt 7387 lies in the middle of stem S1 of the predicted PK structure suggests that PK formation is impaired in 3NC202 at 39.5°C and that as a result, RNA synthesis may be impaired.

To test this hypothesis, revertants of 3NC202, which appeared at the low frequency of 2×10^{-4}, were isolated and their genotypes were determined. Eight revertants of 3NC202 were isolated from individual plaques formed on HeLa cell monolayers at 39.5°C and were plaque purified three times. To confirm that these viruses were functional revertants, viral RNA synthesis was monitored in HeLa cells at 39.5°C, revealing that the revertant viruses synthesized RNA with kinetics similar to those of wild-type virus (data not shown).

The 3′ NCR nucleotide sequences of 8 revertants fell into

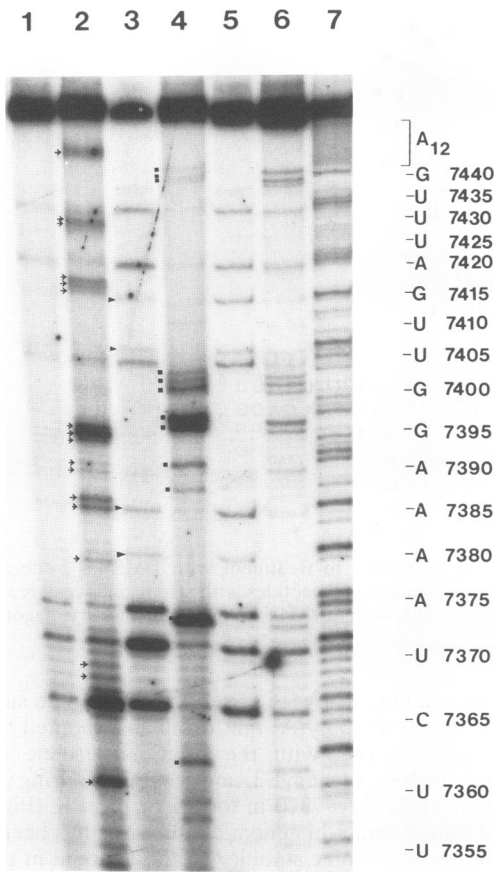

FIG. 5. Enzymatic probing of in vitro-synthesized, 5′-end-labeled poliovirus RNA. ^{32}P-end-labeled T7-WT S/E pA RNA [132-nt poly(A)$_{12}$ RNA (Fig. 2B)] was treated with nucleases as described in Materials and Methods. The reaction products were then analyzed on a urea-containing polyacrylamide gel, and an autoradiograph of a representative gel is shown. Lanes: 1, untreated RNA; 2, V1 (→); 3, RNase A (▲); 4, RNase T_1 (■). Sequencing of the RNA was performed as described in Materials and Methods. Lanes: 5, untreated; 6, RNase T_1 (G specific); 7, RNase PhyM (A>U specific). The identity of every fifth nucleotide and its nucleotide number are indicated on the right.

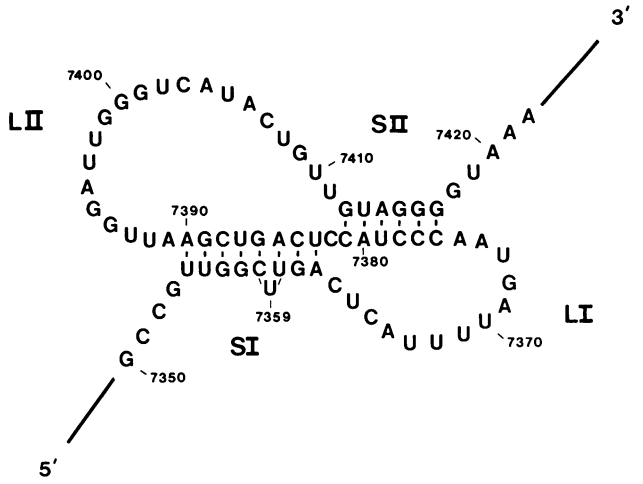

FIG. 6. Predicted PK structure located at the 3′ terminus of the poliovirus genome. S, stem; L, loop.

four sequence classes with striking similarities among them (Fig. 7). Each revertant had deleted 7 or 8 contiguous nt composed of both wild-type and mutant 3NC202 sequences. All of the revertants deleted wild-type G-7386 and U-7387 (top of stem element II in Fig. 4) plus the linker sequence CGGUU (R3 and R9) or CGGUUA (R1, R2, R4, R5, R7, and R8). This resulted in a 2- or 3-nt substitution, respectively, of wild-type G-7386 and U-7387 to revertant AC or AAC. Accordingly, the R3 and R9 mutations resulted in the net addition of 1 nt compared with the wild type. All revertants thus retained element I of the hairpin stem, although the top of the stem (element II, Fig. 4) is probably destabilized by the AC or AAC revertant sequence replacing the wild-type GU sequences. Some revertants also had an A-7406-to-G mutation which could potentially base pair with the revertant C residue across the top of the stem. Importantly, all of these revertants could potentially restore base pairing in stem S1 of the pseudoknot, although with different base-pairing partners for G-7357 and U-7359. Six of the revertants could form a wild-type-like PK (containing a single bulged C residue in stem I), while the PK in R9 should contain a symmetrical loop of 2 nucleotides and R3 should restore stem S1 without any bulged nucleotides.

Viral RNA synthesis correlates with PK formation. To test the hypothesis that the linker insertion in 3NC202 blocked RNA synthesis at 39.5°C because of a change in local RNA structure, the structure of T7-3NC202 pA was analyzed by chemical and enzymatic probing with primer extension. The in vitro transcript was similar to T7-WT B/S pA (Fig. 2), except for the 8-nt insertion at nt 7387. Figure 8 shows that the secondary structure downstream of G-7394 was similar to that of the wild type. The DMS- and RNase A-sensitive sites (lanes 2 and 4) between nt 7403 and 7406 and at U-7419, plus the T_1-sensitive sites at residues G-7399/G-7400, G-7394/G-7395, and G-7389 (lane 5), were present, indicating that the basic stem-loop structure remained intact. This is further supported by the reactivities of U-7370, G-7372, and U-7373 (lanes 4 and 5) upstream of the hairpin that are the same as those in wild-type RNA. However, V1 sites associated with PK formation near the insertion site at C-7388/G-7389 and at A-7385 were missing (lane 3), indicating that stem S1 formation of the PK was impaired. Additionally, the U-4 stretch (nt 7367 to 7370, lane 4) was less susceptible to V1 and shows only one reactive site compared with three in wild-type RNA. In several experiments, this V1 site was clearly absent, while the rest of the probing pattern was consistent.

Next, the RNA secondary structure of 3′-terminal revertant RNA transcripts was examined. The structural analysis of several revertant 3′ NCRs showed them to be very similar to one another and to the wild type. Figure 9 shows a representative autoradiogram of the structure analysis of revertant R9. The R9 transcript (T7-R9 B/S pA) contained the revertant nucleotide changes AAC (at the top of the hairpin stem which replaced the wild-type residues G-7386 and U-7387) plus the A-to-G transition at nt 7406. The essential feature of the banding pattern is that R9 regained the V1 hits at A-7385 and C-7388 (lane 3), characteristic of PK formation, thereby restoring a V1 reactivity pattern identical to that for wild-type RNA (compare lanes 3 of Fig. 3 and 10). Additionally, the revertant AAC triplet was not susceptible to DMS or RNase A, consistent with the base pairing of these nucleotides in S1 of the PK. In fact, the PK

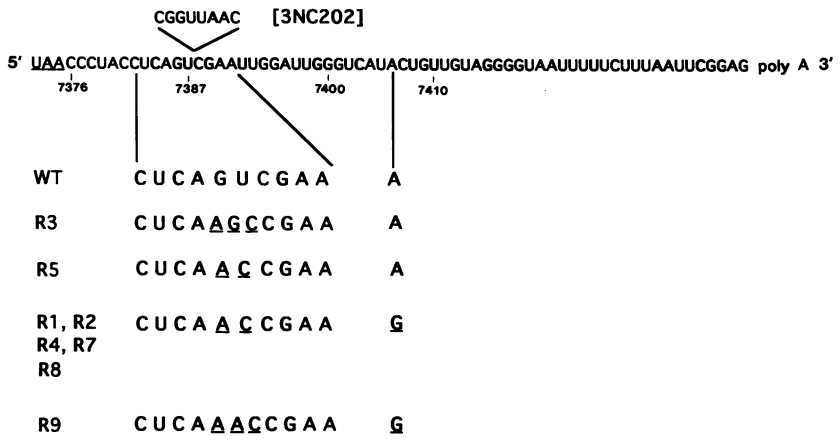

FIG. 7. Nucleotide sequence of the 3′ NCRs of wild-type, mutant 3NC202, and revertant polioviruses. (Top) Wild-type 3′ NCR. The stop codon used to terminate translation is underlined. The 8-nt insertion at position 7387 in mutant 3NC202 is shown above. (Bottom) Nucleotides 7382 to 7392 and 7406 of the wild type and 8 revertant genomes are enlarged to show the sequence changes of revertants (underlined).

conformation may be favored over the hairpin in R9 relative to the wild type because of the destabilization of the top 2 base pairs of element II of the hairpin, which may destabilize this entire element.

Recently, Pilipenko et al. (23) suggested that nt 7388 to 7393 could form a higher-order structure by base pairing with nt 7432 to 7437 as opposed to nt 7354 to 7362, as reported here. However, this observation is not supported by experimental data because nt 7432 to 7437 were not susceptible to cleavage by both single-strand-specific and helical nucleases (23) (Fig. 4), and the restoration of element II in the revertant genotypes favors base pairing of nt 7388 to 7393 with nt 7354 to 7362 instead of 7432 to 7437.

Site-directed mutagenesis of the proposed PK. Finally, we tested the existence of stem S1 in the RNA PK by site-directed mutagenesis of the residues involved in the formation of S1. Figure 10 shows the sequence of mutant PK1pA that contains nt AACCCAAUAU in place of wild-type U-7354–UGGCUUGAC–7363, which should disrupt base pairing between these two regions and, thus, that of stem S1. One additional uridine residue was inserted at nt 7367 to create a unique restriction endonuclease site for screening during cloning, and it is not expected to exert a structural influence because of its position in loop I of the PK.

In vitro structure analysis of 5′ ^{32}P-labeled PK1pA RNA transcripts was performed, and the reactivities of nt 7350 to 7420 to biochemical probes are shown mapped onto the hairpin structure (Fig. 10). Consistent with the loss of PK formation, PK1pA displayed a loss of V1 sites at U-7360, C-7365, U-7367 to U-7370, and G-7389 and gained new RNase A-susceptible sites in this region at C-7358, U-7361, and C-7365. Loss of V1 reactivity at U-7367 to U-7370 may be due to diminished pairing of these sequences with 3′-terminal poly(A) residues. This pairing could have been favored when sequences from U-7367 to U-7370 were displayed in loop I of the proposed PK (Fig. 6). Furthermore, new V1 sites at G-7353 and A-7366 indicate that this mutant RNA may have a novel folding conformation upstream of the 3′ NCR, although the hairpin stem is apparently unaffected, as demonstrated by the wild-type-like V1 sites at C-7378, C-7384/A-7385, and G-7415. These data are consistent with PK disruption in PK1pA and provide, together with the genotypes of the revertant genomes, further evidence for the existence of stem S1 in the proposed PK.

Phylogenetic analysis of related picornaviruses reveals that a similar PK can be formed in coxsackievirus B1. If the PK structure plays a functional role in the poliovirus infectious cycle, one would expect this structure to be conserved among related picornaviruses. The 3′ NCR sequences of the various strains of poliovirus are highly conserved (38). Comparison of the 3′ NCR of poliovirus to those of other picornaviruses, displaying different tissue tropism such as encephalomyocarditis virus and human rhinovirus, does not reveal significant sequence similarity for structures with potentially similar functions to be aligned. However, the 3′ NCR of coxsackievirus B1 (14), a member of the enteroviruses like poliovirus, shows both sequence and structure similarity to the 3′ NCR of poliovirus. Figure 11 shows the minimal-energy RNA folding of the 3′ NCR of coxsackievirus B1 that bears a close resemblance to that of poliovirus in several respects. First, there is a predicted RNA hairpin structure that features 6 bp in the bottom half of the stem and 4 bp in the top half of the stem separated by a small internal loop. In addition, coxsackievirus B1 contains an insertion of 36 nt between the UAA translation termination codon and the RNA hairpin; this 36-nt insertion can be folded into another RNA hairpin structure. As a result, the 3′-terminal coding sequence of 3D polymerase can be brought into as close proximity to the first RNA hairpin as that in the 3′ NCR of poliovirus (Fig. 3). Accordingly, the coxsackievirus B1 loop sequences 5′-CUAACCG-3′ could base pair with the upstream sequences 5′-UGGUUGG-3′, forming a PK very similar to that of poliovirus (Fig. 6). That contiguous RNA sequences can be folded to bring together two functional sequence elements that are linearly distant from each other has been observed previously with other viral genomes: human T-cell leukemia virus type 1 brings together two linearly distant RNA sequences by looping out the *rex*-responsive element to create a functional polyadenylation signal (1). Furthermore, the sequences 5′-ACUCUUUUU-3′, located between the upstream PK S1 donor sequences and the RNA hairpin, would form loop I in the PK, as seen in the PK in the poliovirus genome. Similarly, the uridine residues located upstream of the coxsackievirus B1 translational stop codon could be engaged in base pairing with the poly(A) tail. An ultimate test for a role of the proposed coxsackievirus B1 PK structure in viral RNA amplification could be demonstrated by the successful isolation of chi-

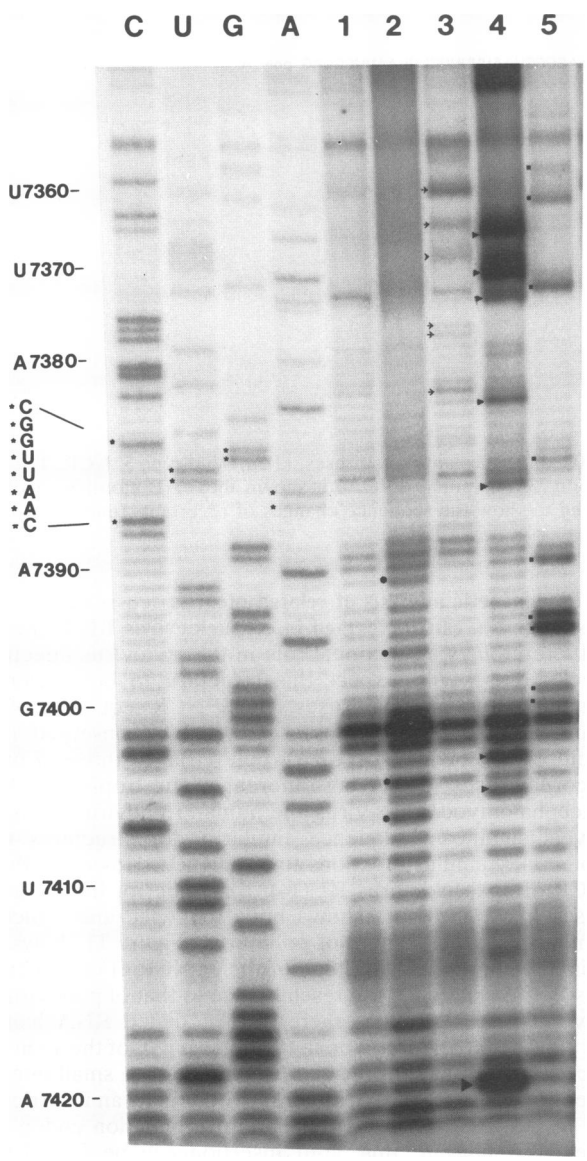

FIG. 8. Structural analysis by chemical and enzymatic probing of mutant 3NC202 poliovirus RNA. T7-3NC202 B/S pA RNA was treated and analyzed as described in the legend to Fig. 3. Lanes: 1, untreated RNA; 2, DMS (●); 3, V1 (→); 4, RNase A (▲); 5, RNase T_1 (■). Nucleotides marked with stars represent the 8-nt insertion in 3NC202.

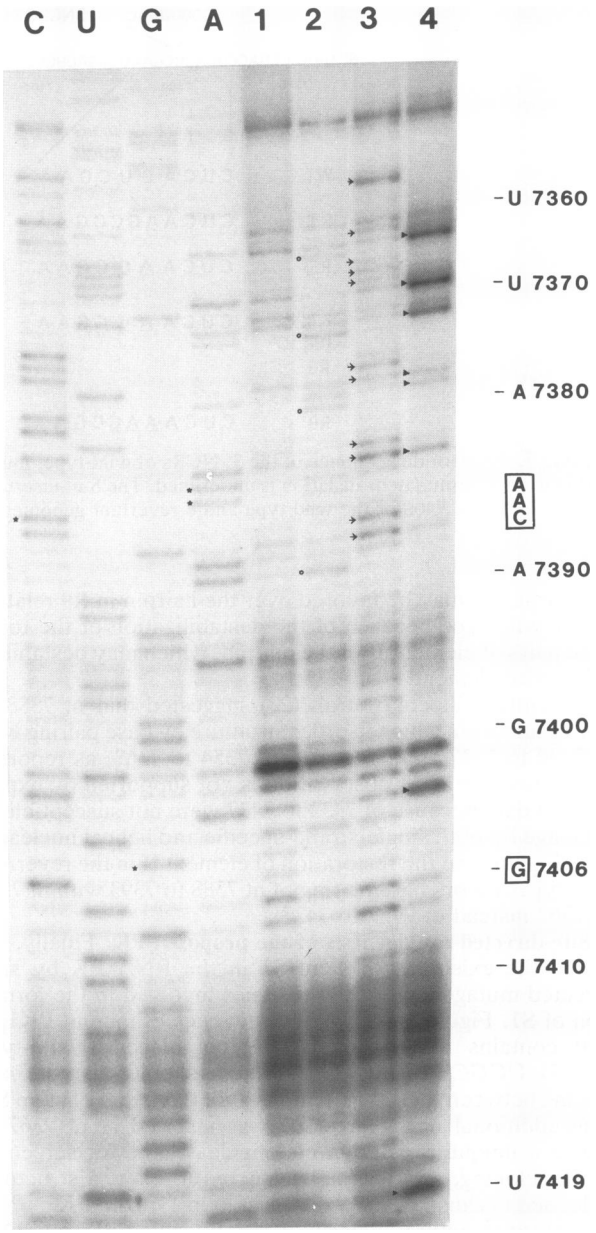

FIG. 9. Structural analysis by chemical and enzymatic probing of revertant R9 poliovirus RNA. T7-R9 B/S pA RNA was treated and analyzed as described in the legend to Fig. 3. Lanes: 1, untreated RNA; 2, DMS (○); 3, V1 (→); 4, RNase A (▲). Nucleotide changes in the revertant genome with respect to that of the wild type are boxed (right) or marked with stars in the sequencing lanes.

meric polioviruses bearing the proposed coxsackievirus B1 PK structure in their 3′ NCRs.

DISCUSSION

We have provided evidence for an RNA PK at the 3′ terminus of genomic, plus-sense poliovirus RNA. This PK apparently exists in equilibrium with a simpler stem-loop structure beginning just downstream of the termination codons. Thermodynamic-based RNA structure calculation, combined with chemical and enzymatic structure probing of in vitro-transcribed RNA molecules, allowed us to analyze the secondary structure of the 3′-terminal 100 nt of poliovirus RNA. We found that most of the RNA residues that were susceptible to modification were recognized exclusively as either single-stranded or helical, thereby defining a primary RNA hairpin extending from nt 7376 to 7417. Interestingly, several residues (e.g., C-7388, G-7389, and G-7394) reacted strongly with DMS or T_1, probes for single-stranded conformation, as well as with V1, a probe for helical RNA structure. This raised the possibility that a higher-order base-pairing interaction may exist as an alternative conformation, forming a PK in which nt 7383 to 7390 are base paired with nt 7354 to 7362.

A genetic analysis was subsequently performed to assess the functional significance of the poliovirus 3′-terminal PK in

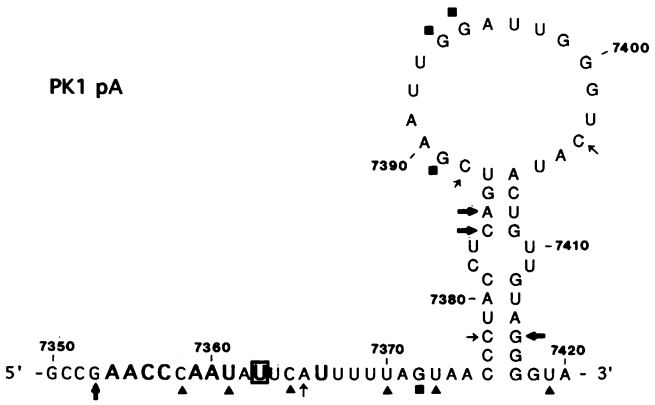

FIG. 10. Structure analysis of mutant RNAs bearing defined nucleotide changes in stem S1 of the proposed PK. An RNA transcript containing mutated residues (bold) upstream of the 3′ NCR (designated PK1pA) containing a 5′-terminal ^{32}P was subjected to enzymatic probing. Reactivities of nt 7350 to 7420 are shown mapped onto the stem-loop structure shown in Fig. 4. Cobra venom nuclease V1 (➡), RNase A (▲), and RNase T_1 (■) are marked. Strong reactivity is denoted by thick arrows, and weak reactivity is denoted by thin arrows. The extra U residue (boxed) in the RNA chain resulted from sequences in the DNA specifying a restriction enzyme site.

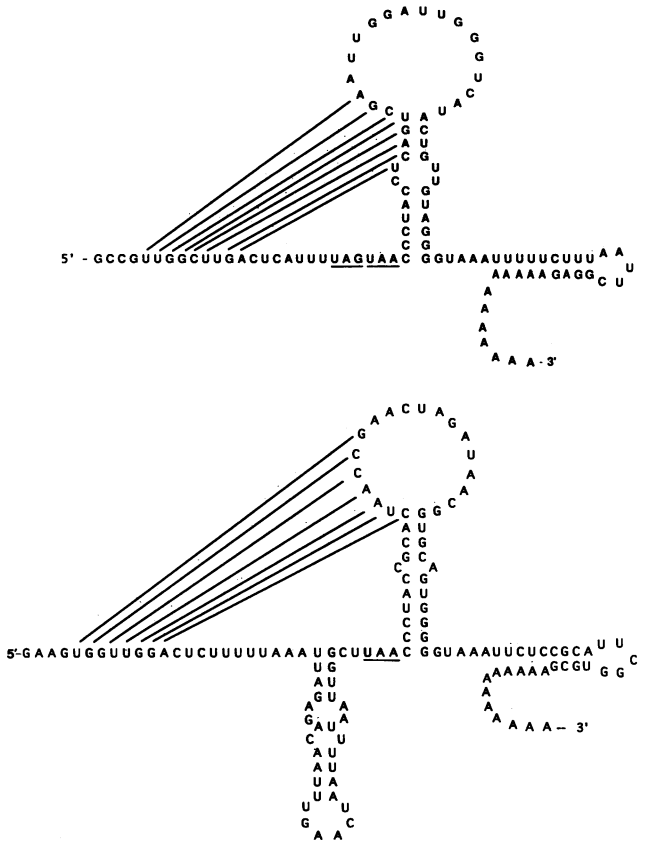

FIG. 11. Predicted structures at the 3′ termini of wild-type poliovirus RNA (top) and coxsackievirus B1 RNA (bottom). Translational termination codons are underlined. Diagonal lines illustrate potential base-pairing interactions between nucleotides.

the virus life cycle. Revertants of an existing poliovirus mutant (3NC202), which bears an 8-nt insertion in stem S1 of the proposed PK in the 3′ NCR and displayed a temperature-sensitive phenotype for viral RNA synthesis, were isolated, and their genotypes were determined. All revertants exhibited restored RNA synthesis at the temperature nonpermissive for the mutant 3NC202. Eight revertants had sequence alterations in the region of the insertion in the 3′ NCR that could potentially restore base pairing in the PK. RNA secondary structure analysis by chemical and enzymatic probing of mutant (3NC202) and revertant (R9) 3′-terminal RNA transcripts demonstrated that PK formation was impaired in 3NC202 RNA and restored in the revertant RNA molecules, which correlated with the observed functional properties of the mutant and revertant genomes in vivo.

The importance of PK structures has been suggested for functionally diverse RNA molecules (8; for a review, see reference 24). First, PK structures have been implicated in regulating translation initiation of prokaryotic RNA by mediating the binding of translational repressor proteins (19, 36). There is no evidence to suggest that a PK in the poliovirus 3′ NCR may influence translation of the viral genome. However, the viral RNA is polyadenylated, and several studies have previously demonstrated a role for the poly(A) tail as well as the poly(A)-binding protein in cellular mRNA translation (13, 30). Binding of the poly(A)-binding protein to poliovirus RNA has not been demonstrated, but poly(A)-binding protein–RNA interactions may influence the 3′-terminal RNA structure of genomic sense RNA or possibly participate in the viral replication initiation complex.

Second, PKs have been found to direct ribosomal frameshifting in several viruses to produce a viral RNA-dependent DNA polymerase via a *gag-pol* fusion protein encoded in overlapping reading frames. The mechanism of frameshifting is thought to include two RNA elements: a slippery sequence, UUUAAAC (7) or UUUA (15), upstream of the frameshift site and a stable hairpin or PK just downstream of the frameshift site. If the poliovirus PK has a similar function, a viral polymerase could be generated with extra carboxy-terminal residues, which could confer a specialized function.

A third role of PK structures is the formation of active sites in self-cleaving RNAs such as group I introns and RNase P (reviewed in reference 24) as well as hepatitis delta virus RNA (22). There is evidence that the small peptide VPg, covalently bound to the 5′ end of poliovirus RNA in infected cells, could be attached to the 5′ end of the viral minus strand by a *trans* esterification reaction reminiscent of autocatalytic RNAs (37). Because this reaction was shown to be specific to poliovirus RNA, higher-order RNA folding at the 3′ end may be part of an active site, enabling this to occur.

Specific higher-order structures at the 3′ end of RNA molecules have been proposed to constitute replication signals that are responsible for the selective amplification of RNA molecules (39). For example, many plus-stranded RNA viruses are known to contain 3′-terminal tRNA-like structures that bind proteins involved in tRNA metabolism and aminoacylation (29). Also, prokaryotic bacteriophages such as Qβ contain a 3′-terminal tRNA-like CCA which recruits proteins of the cellular translational machinery to replicate their genomes (6). Poliovirus may have acquired an analogous function in which the terminal PK can function as a nucleation site for the assembly of the viral replication complex by binding the viral polymerase or a cellular factor

involved in selective amplification of the viral genome or both.

The precise mechanism of amplification of poliovirus RNA in infected cells is not known. Two models have been proposed: an RNA snapback model and a VPg priming model. The central feature of the snapback model is that the genetically encoded poly(A) tail is uridylated, creating a self-complementary A_nU_n structure. The poly(U) tract could then serve as a primer for the viral polymerase to initiate minus-sense RNA synthesis (reviewed in reference 28). The central feature of the VPg priming model is that a uridylated form of the VPg protein could itself act as a primer for the initiation of RNA synthesis (reviewed in reference 28). The participation of the PK structure in the initiation of minus-strand RNA would fit either model. Interestingly, the 3′ end of the minus-strand RNA, where the initiation of positive-strand RNA must occur, has been previously shown to contain a cloverleaf-like RNA structure (2). Therefore, different types of higher-order RNA structures on both ends of the viral genome may dictate the specific amplification of the viral RNA in mammalian cells by either of the proposed mechanisms.

ACKNOWLEDGMENTS

We thank Erika Norris for help in sequencing and reconstruction of revertants of 3NC202. We are grateful to Karla Kirkegaard for critical comments on the manuscript.

This work was supported by Public Health Service grants AI-25105 (P.S.) and NS-07321 (S.J.J.) from the National Institutes of Health and in part by a grant from the Lucille P. Markey Charitable Trust. P.S. acknowledges the receipt of a Faculty Research Award from the American Cancer Society.

REFERENCES

1. **Ahmed, Y. F., G. M. Gilmartin, S. M. Hanly, J. R. Nevins, and W. C. Greene.** 1991. The HTLV-1 Rex response element mediates a novel form of mRNA polyadenylation. Cell **64**:727–737.
2. **Andino, R., G. E. Rieckhof, and D. Baltimore.** 1990. A functional ribonucleoprotein complex forms around the 5′ end of poliovirus RNA. Cell **63**:369–380.
3. **Auron, P. E., L. D. Weber, and A. Rich.** 1982. Comparison of transfer ribonucleic acid structures using cobra venom and S_1 endonucleases. Biochemistry **21**:4700–4706.
4. **Ausubel, F. M., R. Brent, R. E. Kingston, D. D. Moore, J. G. Seidman, J. A. Smith, and K. Struhl.** 1989. Current protocols in molecular biology. Wiley Interscience, New York.
5. **Bernstein, H. D., P. Sarnow, and D. Baltimore.** 1986. Genetic complementation among poliovirus mutants derived from an infectious cDNA clone. J. Virol. **60**:1040–1049.
6. **Blumenthal, T. B., and G. G. Carmichael.** 1979. RNA replication function and structure of Qβ replicase. Annu. Rev. Biochem. **48**:525–548.
7. **Brierley, I., P. Digard, and S. C. Inglis.** 1989. Characterization of an efficient coronavirus ribosomal frameshifting signal: requirement for an RNA pseudoknot. Cell **57**:537–547.
8. **Chastain, M., and I. Tinoco, Jr.** 1991. Structural elements in RNA. Prog. Nucleic Acid Res. Mol. Biol. **11**:131–177.
9. **Dalbadie-McFarland, G., L. W. Cohen, A. D. Riggs, C. Morin, K. Itakura, and J. H. Richards.** 1982. Oligonucleotide-directed mutagenesis as a general and powerful method for studies of protein function. Proc. Natl. Acad. Sci. USA **79**:6409–6413.
10. **Dasgupta, A., P. Zabel, and D. Baltimore.** 1980. Dependence of the activity of the poliovirus replicase on a host cell protein. Cell **19**:423–429.
11. **Donis-Keller, H.** 1980. Phy M: an RNAse activity specific for U and A residues useful in RNA sequence analysis. Nucleic Acids Res. **8**:3133–3142.
12. **Flanegan, J. B., and T. A. Van Dyke.** 1979. Isolation of a soluble and template-dependent poliovirus RNA polymerase that copies virion RNA in vitro. J. Virol. **32**:155–161.
13. **Gallie, D. R.** 1991. The cap and poly(A) tail function synergistically to regulate mRNA translational efficiency. Genes Dev. **5**:2108–2116.
14. **Iizuka, N., S. Kuge, and A. Nomoto.** 1987. Complete nucleotide sequence of the genome of coxsackievirus B1. Virology **156**:64–73.
15. **Jacks, T., H. D. Madhani, F. R. Masiarz, and H. E. Varmus.** 1988. Signals for ribosomal frameshifting in the Rous sarcoma virus gag-pol region. Cell **55**:447–458.
16. **Jaeger, J. A., D. H. Turner, and M. Zuker.** 1989. Improved predictions of secondary structures for RNA. Proc. Natl. Acad. Sci. USA **86**:7706–7710.
17. **Kitamura, N., B. L. Semler, P. G. Rothberg, G. R. Larsen, C. J. Adler, A. J. Dorner, E. A. Emini, R. Hanecak, J. J. Lee, S. van der Werf, C. W. Anderson, and E. Wimmer.** 1981. Primary structure, gene organization and polypeptide expression of poliovirus RNA. Nature (London) **291**:547–553.
18. **Lowman, H. B., and D. E. Draper.** 1986. On the recognition of helical RNA by cobra venom V_1 nuclease. J. Biol. Chem. **261**:5396–5403.
19. **McPheeters, D. S., G. D. Stormo, and L. Gold.** 1988. Autogenous regulatory site on the bacteriophage T4 gene 32 messenger RNA. J. Mol. Biol. **201**:517–535.
20. **Moazed, D., S. Stern, and H. F. Noller.** 1986. Rapid chemical probing of conformation in 16S ribosomal RNA and 30S ribosomal subunits using primer extension. J. Mol. Biol. **187**:399–416.
21. **Pelletier, J., and N. Sonenberg.** 1988. Internal initiation of translation of eukaryotic mRNA directed by a sequence derived from poliovirus RNA. Nature (London) **334**:320–325.
22. **Perrotta, A. T., and M. D. Been.** 1991. A pseudoknot-like structure required for efficient self-cleavage of hepatitis delta virus RNA. Nature (London) **350**:434–436.
23. **Pilipenko, E. V., S. V. Maslova, A. N. Sinyakov, and V. I. Agol.** 1992. Towards identification of cis-acting elements involved in the replication of enterovirus and rhinovirus RNAs: a proposal for the existence of tRNA-like terminal structures. Nucleic Acids Res. **20**:1739–1745.
24. **Pleij, C. W. A.** 1990. Pseudoknots: a new motif in the RNA game. Trends Biochem. **15**:143–147.
25. **Pleij, C. W. A., K. Rietvald, and L. Bosch.** 1985. A new principle of RNA folding based on pseudoknotting. Nucleic Acids Res. **13**:1717–1731.
26. **Puglisi, J. D., J. R. Wyatt, and I. Tinoco, Jr.** 1988. A pseudoknotted RNA oligonucleotide. Nature (London) **331**:283–286.
27. **Racaniello, V. R., and D. Baltimore.** 1981. Molecular cloning of poliovirus cDNA and determination of the complete nucleotide sequence of the viral genome. Proc. Natl. Acad. Sci. USA **78**:4887–4891.
28. **Richards, O. C., and E. Ehrenfeld.** 1990. Poliovirus RNA replication. Curr. Top. Microbiol. Immunol. **161**:89–119.
29. **Rietvald, K., C. W. A. Pleij, and L. Bosch.** 1983. Three-dimensional models of the tRNA-like 3′ termini of some plant viral RNAs. EMBO J. **2**:1079–1085.
30. **Sachs, A., and R. Davis.** 1989. The poly(A) binding protein is required for poly(A) shortening and 60S ribosomal subunit-dependent translation initiation. Cell **58**:857–867.
31. **Sarnow, P.** 1989. Role of 3′-end sequences in infectivity of poliovirus transcripts made in vitro. J. Virol. **63**:467–470.
32. **Sarnow, P., H. D. Bernstein, and D. Baltimore.** 1986. A poliovirus temperature-sensitive RNA synthesis mutant located in a noncoding region of the genome. Proc. Natl. Acad. Sci. USA **83**:571–575.
33. **Simoes, E. A. F., and P. Sarnow.** 1991. An RNA hairpin at the extreme 5′ end of the poliovirus RNA genome modulates viral translation in human cells. J. Virol. **65**:913–921.
34. **Spector, D. H., and D. Baltimore.** 1974. Requirement of 3′-terminal poly (adenylic acid) for the infectivity of poliovirus RNA. Proc. Natl. Acad. Sci. USA **71**:2983–2987.
35. **Stern, S., D. Moazed, and H. Noller.** 1988. Analysis of RNA

structure using chemical and enzymatic probing monitored by primer extension. Methods Enzymol. **164:**481–489.

36. **Tang, C. K., and D. E. Draper.** 1989. Unusual mRNA pseudoknot structure is recognized by a protein translational repressor. Cell **57:**531–536.
37. **Tobin, G. J., D. C. Young, and J. B. Flanegan.** 1989. Self-catalyzed linkage of poliovirus terminal protein VPg to poliovirus RNA. Cell **59:**511–519.
38. **Toyoda, H., M. Kohara, Y. Kataoka, T. Suganuma, T. Omata, N. Imura, and A. Nomoto.** 1984. Complete nucleotide sequences of all three poliovirus serotype genomes. Implication for genetic relationship, gene function and antigenic determinants. J. Mol. Biol. **174:**561–585.
39. **Weiner, A. M., and N. Maizels.** 1987. tRNA-like structures tag the 3′ ends of genomic RNA molecules for replication: implications for the origin of protein synthesis. Proc. Natl. Acad. Sci. USA **84:**7383–7387.
40. **Zaug, A. J., J. R. Kent, and T. R. Cech.** 1984. A labile phosphodiester bond at the ligation junction in a circular intervening sequence RNA. Science **224:**574–578.
41. **Zuker, M.** 1989. On finding all suboptimal foldings of an RNA molecule. Science **244:**48–52.